

# VIRTUAL TEST BENCH TO CHARACTERIZE LOAD BEARING BEHAVIOR OF LAMINATES WITH OUT-OF-PLANE PLY DEFLECTIONS AND LOCALIZED WRINKLES

Swami S. Venkat<sup>1</sup>, Mathias P. Hartmann<sup>1</sup>

<sup>1</sup>Chair for Carbon Composites, TUM Department of Mechanical Engineering, Technical University of  
Munich, Boltzmannstraße 15, 85748 Garching, Germany

Email: venkat@lcc.mw.tum.de, Web Page: <http://www.lcc.mw.tum.de/startseite/>

**Keywords:** ply undulations, wrinkles, graded waviness, progressive failure, delamination, continuum damage, cohesive elements

## Abstract

This study initially focuses on the methodologies developed for the fabrication of carbon fiber reinforced laminates with graded out-of-plane ply waviness and with localized folding or wrinkling of a ply. Literature review has shown that there have been methods developed to fabricate laminates with similar defects. In this study the localized wrinkle defect in a ply is introduced using temporary insertion of a rod and the graded waviness is introduced using the bent plate method. Critical parameters which influence the severity of the generated defect have been investigated and the most relevant results are presented. Special emphasis is laid on the simplicity and reproducibility of the two methods. Second part of the study focuses on a virtual test bench, which is developed using Python based application process interface (API) in Abaqus FEA to reproduce the defect geometry in a finite element (FE) environment. Analysis of the progressive failure in the plies is performed in Abaqus using a continuum damage model and cohesive elements to track the formation and growth of delamination at ply interfaces. The simulation of specimens featuring the ply waviness have been performed under static tensile and compressive load cases. As expected, the presence of ply undulations leads to an earlier onset of damage due to delamination between undulated plies. In extreme cases the maximum load that the laminate can bear has seen a drop of more than 60%.

## 1. Introduction

### 1.1. Background

The weight saving potential of carbon fiber reinforced plastic materials has made them a preferred choice for high performance components in the aeronautical industry. Efficient manufacturing techniques involve the layup and draping of dry preforms on complex geometries followed by a resin infusion or injection process with subsequent cure. Limited in-plane deformability particularly in shear may result in out-of-plane ply waviness or even wrinkles when forming compound curved shapes and especially during the consolidation phase when high in-plane compressive forces may arise exceeding the critical buckling load of the preforms [1]. Fig. 1 shows a so called 'graded waviness' type of defect in the laminate where there is gradient of amplitude to defect length ratio of the successive plies through the thickness. Such defects arise due to thickness change in hinge point area and it is an example of defect induced during the compaction phase. Kugler and Moon [2] found out that the tool plate/part coefficient of thermal expansion (CTE) mismatch can result in in-plane and out-of-plane waviness in a laminate. This is due to the fact that longitudinal CTE of the laminate is negative and it expands while cooling while that of metal tools like aluminium is positive and it contracts while cooling. In thick laminates it can affect the skin layers of the laminate. In the same paper [2] the effect of cooling rate has also been investigated since rapid cooling of the laminate can cause temperature gradients through the thickness of the laminate and therefore difference in volumetric contractions

leading to waviness on surface. These manufacturing induced defects are highly detrimental to the mechanical performance and service life of composite parts and hence there is a need for thorough investigation of their effect on the structural integrity of the components.

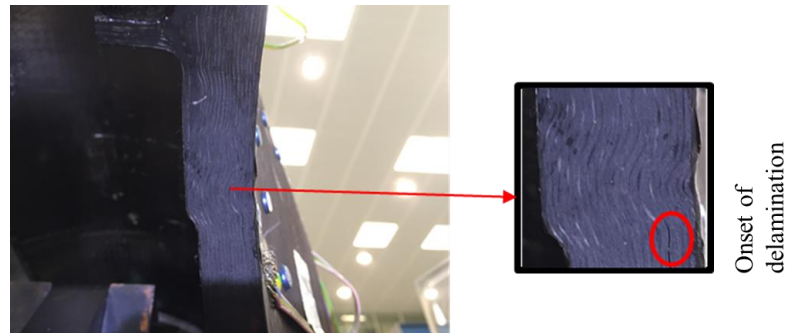


**Figure 1.** Out-of-plane graded waviness in an aerospace R&T component

Literature [3,4,5,6,7] show that different methods have been used to artificially induce waviness or ply folding defects in a laminate and characterize them on coupon level to study their impact on stiffness and strength. Wisnom et. al. [3] created samples with waviness by creating a layup on curved plate and straightening it before curing. Wang et. al. [4] developed transverse strip and ply drop methods to generate two representative waviness configurations. Hörrmann et. al. [6] has shown that defects like ply folding cannot be avoided during high pressure resin transfer molding process and used unidirectional (UD) samples with such defects to study the fatigue behavior. They concluded that folds have minor influence on the fatigue performance of UD laminates but in multidirectional laminates the waviness introduced in the subsequent plies due to folds can reduce the compression strength and fatigue life by 50%. In a study conducted by Adams and Hyer [7], waviness was introduced in an isolated layers in center of the laminate in an otherwise undisturbed laminate with defect amplitude to length ( $\delta/l$ ) ratios varying from 0.023 to 0.077 and the compression tests on these laminates showed a strength drop of between 1 to 36%.

The analytical or numerical modeling of such defects have also been a subject of study of several researchers. Bogetti et al. [8] developed an analytical model to investigate the effects of layer waviness on the stiffness and strength reduction of a composite laminate, but without any comparison to test data. Hsiao et. al. [9] also developed an analytical model to determine the elastic properties as a function of fiber waviness and also strength predictions using maximum stress and Tsai-Wu criteria. This study also included fabrication of plates with waviness, compression tests on these samples and the comparison of test results with the results of analytical methods. However a limitation of analytical methods in literature is that they use classical lamination theory for the development of such models which assumes a perfect bonding between the plies and not cohesive nature of the interfaces. There have also been investigations using wavy FE representative unit cells [10] to predict the smeared orthotropic stiffness and failure in a lamina featuring waviness. But such methods are applicable only at the ply level and cannot be used to predict the laminate behavior with delamination at the ply interfaces. Therefore, this study is inspired by works of Lemanski et. al. [11] and doctoral work of Duangmuan [12], in which a detailed FE modelling approach is used including cohesive elements to model the delamination between the plies. In [11] and [12] a good prediction of failure modes and the load levels were achieved with respect to the test results.

## 1.2. Approach

The literature survey shows that the anomalies in laminates like the graded waviness shown in Fig. 1 and the localized wrinkle defects have not been addressed in detail until now. These kind of defects and their effects on the stiffness and strength of laminates are the focus of the work at hand. First, the fabrication techniques are presented for generating representative defects in the laminates. An FE

based simulation approach is presented to investigate the load response of laminates featuring ply undulations and to track failure progression as well as failure modes during virtual coupon tests. The virtual test bench presented here aims at automatic generation of representative FE models with the information gained from section and microsection images of defect geometries.

## 2. Methods of defect introduction in laminates

Two types of ply undulations have been investigated in this study. The wrinkled defect is introduced in the specimen using a temporary insertion of rod and the graded waviness defect is generated using the bent plate method. The plates are fabricated by vacuum assisted resin infusion (VARI) process using two biaxial non-crimp fabrics (NCFs) of orientations  $0^\circ/90^\circ$  and  $\pm 45^\circ$  and the CR80 resin system.

### 2.1. Wrinkled defect

The schematic diagram below (Fig. 2) illustrates the steps used for creating the wrinkled defect in a laminate. The wrinkled defect is introduced in thin laminates of about 4 mm thickness which is a stack of eight bidirectional NCFs. Two locations are chosen for defect introduction and in each case the defect is introduced in a  $\pm 45^\circ$  NCF to compare the two configurations for the influence they can have on the laminate stiffness and strength.

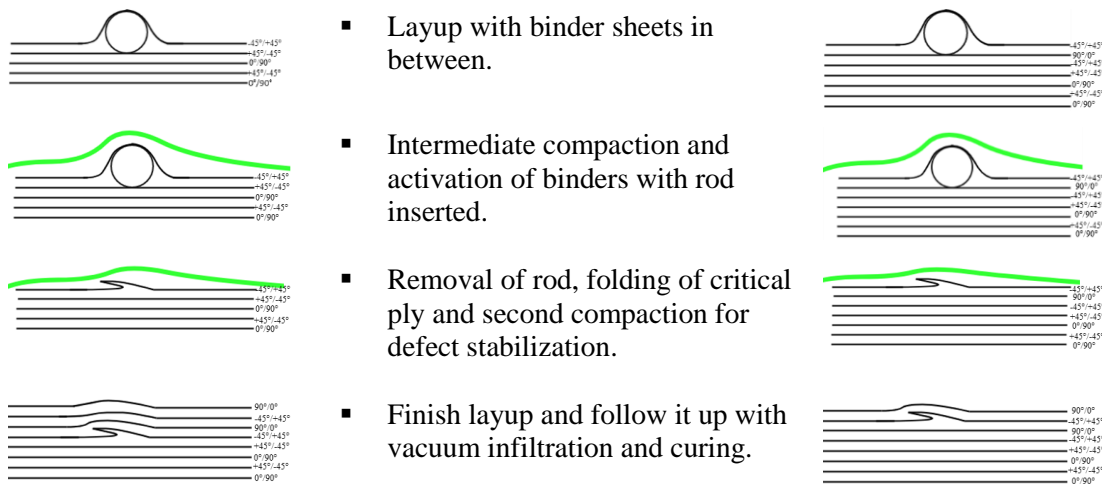


**Figure 2.** Temporary insertion of rod to introduce a wrinkle in a layer of a laminate

The micro sections of the most representative defect geometries are shown below in Fig. 3. These defects were created by inserting a rod of diameter of 15 mm in the laminate. These configurations were identified to be the most relevant among the ones explored. The defect length  $l$  and amplitude  $\delta$  are used for characterizing the defect as indicated in fig. 3b. The defect amplitude to length ratios ( $\delta/l$ ) were measured to values of 2.5 in the first variant and 3.0 in the second variant. The reason for higher value in the second case can be due to the compaction of critical folded layer from the layers above and this results in increase in its amplitude. All the investigations proved that this method is robust and produces reproducible results.

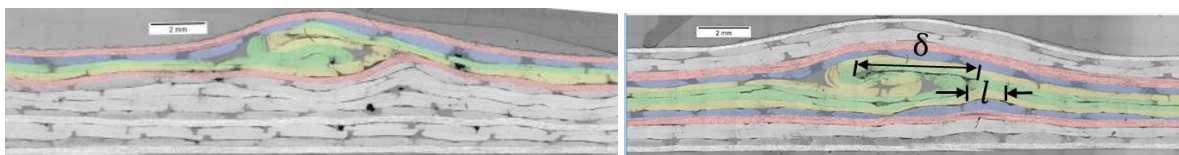


**Figure 3.** Defect creation by temporary insertion of rod method. a) Rod placement before penultimate layer ( $\delta/l=2.5$ ) b) Rod placement in the center of the laminate ( $\delta/l=3.0$ )

## 2.2. Graded waviness

This type of defect can occur as a result of post draping compaction of the perform layup on compound curved tool geometries. During compaction over such curved surfaces, the in-plane axial compression of the preforms can cause waviness formation when their critical buckling load is expected. The bent plate method (Fig. 4) used in this study replicates the in-plane compression of preforms to create laminates with graded waviness. First step in this method is the creation of a layup consisting of two biaxial NCFs with configuration of  $[0^\circ/90^\circ, \pm 45^\circ]_{8s}$  and with binder sheets in between on the bent plate tool. This is followed by intermediate compaction and activation of binders on the tool. The bound laminate is then removed from the tool and vacuum infused and cured on a flat plate. As 32 biaxial NCFs are used, the resulting laminate has a thickness of 16 mm in the undisturbed area.

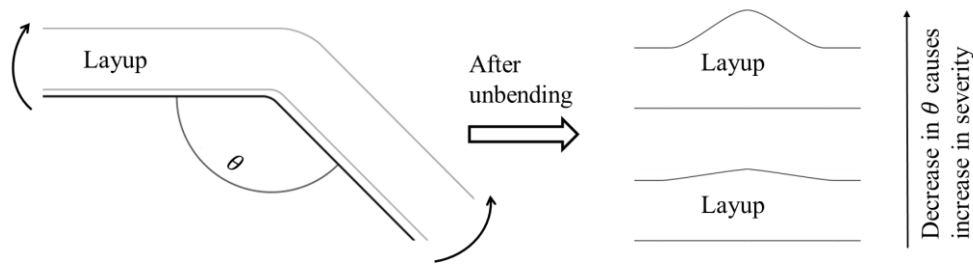


**Figure 4.** Bent plate method to introduce out-of-plane graded waviness in thick laminates

The parameter that influences the defect severity is the flange angle  $\theta$  of the bent plate tool. Among all the investigated samples, the most relevant ones were manufactured on the tools with the flange angles of  $135^\circ$  and  $150^\circ$ . The former produced an amplitude ( $\delta$ ) of 5.0 mm and defect length ( $l$ ) of 20.5 mm on the topmost layer (Fig. 5a) with  $\delta/l$  of 0.243 and the latter produced  $\delta$  of 1.5 mm and  $l$  of 23 mm on the topmost layer with  $\delta/l$  of 0.065. In both the cases the amplitude of the subsequent layers reduce and eventually vanishes at the bottommost layer. In spite of severe nature of  $135^\circ$  variant, it was concluded that these two variants offer a good range of defect amplitude to length ratios which can be used to validate the virtual test bench.

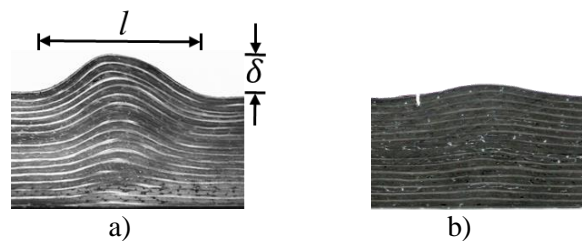


**Figure 5.** Laminates featuring graded waviness introduced with flange angles of a)  $135^\circ$  ( $\delta/l=0.243$ ) and b)  $150^\circ$  ( $\delta/l=0.065$ )

## 3. Finite element simulations

The defects were modeled in Abaqus/Explicit. The reason for this was firstly the problem size as each ply was modeled individually using the 3D continuum shell elements and the interfaces were modeled using cohesive elements. Secondly the non-linearities due to damage modeling could further increase the calculation time dramatically if the implicit method was used and can also cause convergence problems [13].

### 3.1. Graded waviness

#### 3.1.1. Modeling aspects

The simulations were performed on the undisturbed laminates and the laminates featuring graded waviness from the previous section. The specimen geometries for tensile and compression tests planned later are based on standard test methods for composite materials from ASTM [14, 15] and similar studies conducted by Altmann [16]. However for these preliminary simulations the specimen length was limited to 30 mm which covers the entire defect area and a width of 12 mm was taken.

As mentioned in previous chapter these defects were characterized by defect length  $l$  and amplitude of the topmost ply  $\delta$ , so please note that hereafter  $\delta/l$  indicates the maximum defect amplitude to length ratio in a laminate corresponding to the topmost ply. The amplitude of each subsequent ply is reduced by  $\delta/(n-1)$ , where  $n$  is the total number of plies in the laminate and the amplitude therefore vanishes at the bottommost ply. The model is a combination of alternating plies and cohesive sections for modeling the delamination modes. Those two are bound together with tie constraints which link the degrees of freedom of the nodes together. The plies were modeled using reduced integration 8-noded continuum shell SC8R elements and the cohesive sections were modeled using special purpose 8-noded cohesive elements COH3D8. Due to the use of elements with reduced integration formulation, stiffness based hourglass control was used to avoid the occurrence of zero energy modes. By using this control the ratio of artificial energy for curbing the hourglass modes to the total internal energy of the model was kept within 5% as recommended in Abaqus documentation [17]. The boundary conditions are shown in Fig. 6. One side of the specimen is constrained for all degrees of freedom and on the other end velocity boundary condition is applied to a reference point (RP) which has coupling constraint with that end. Though the coupon tests planned later will be done under quasi-static conditions, the velocity value is scaled for the simulations to reduce the computation time. This was made possible as there is no influence of strain rate on material models used in this study.

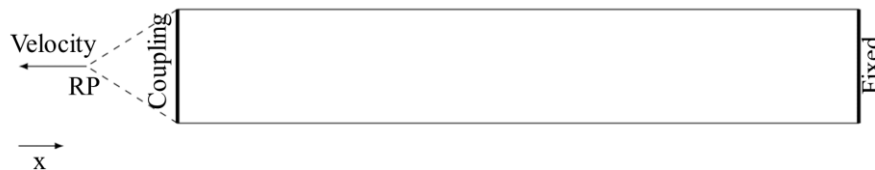


**Figure 6.** Boundary conditions in the FE model

The mechanical response of the plies are modeled using Abaqus anisotropic damage model for composites. It is based on the works of [18, 19, 20, 21]. The onset of damage is based on Hashin criterion [20, 21] which differentiates the four modes of failure (1) fiber rupture in tension (2) fiber buckling and kinking in compression (3) matrix cracking under transverse tension and shear (4) matrix crushing under transverse compression and shearing. The damage evolution is energy based linear softening and controlled by a parameter energy release rate corresponding to each failure mode. The material parameters for the laminates made of HTS fibers infused with RTM6 were used since the characterization tests will be performed on this fiber and resin combination to validate the virtual test bench. The elastic transversely isotropic properties were taken from [22] and the strength values for Hashin criterion and energy release rate parameters for damage evolution were offered from our project partner AIRBUS.

The cohesive interfaces were modeled using the traction-separation implementation in Abaqus. An uncoupled stiffness behavior of the cohesive elements is considered. Energy based damage evolution is defined using the mixed-mode Benzegaggh-Kennane criterion [23], with a linear softening law. The onset of damage is detected using strength values corresponding to a normal fracture mode and two shear fracture modes. The parameters for the cohesive elements were again taken from [22] where a

double cantilever beam (DCB) test was performed based on the norm DIN EN 6033 to determine the parameters for cohesive interface in a HTS/RTM6 laminate. A single lap shear test with cohesive interface between two UD-ply was performed to see the influence of mesh size on the results. The study showed that mesh size had a very pronounced effect on the failure load of the cohesive interface with convergence at a mesh size of 0.5 mm but the stiffness was not influenced by mesh size. Similar studies were done in [22] on DCB specimen which also yielded a mesh convergence at 0.5 mm. Based on [24] it was inferred that the cohesive zone length which depends inversely on the square of strength value influences the mesh size and that if this length is increased then the mesh size can also be made coarser accordingly. The cohesive zone length was increased in this model by decreasing the strength value and mesh size was consequently made coarser to 3 mm. By doing so the computation effort was reduced significantly.

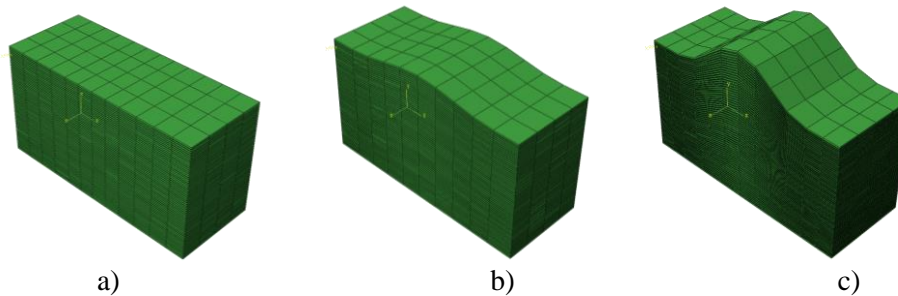


**Figure 7.** FE models of coupons a) Undisturbed b) Graded waviness created with flange angle of  $150^\circ$  ( $\delta/l=0.065$ ), c) Graded waviness created with flange angle of  $135^\circ$  ( $\delta/l=0.243$ )

### 3.1.2 Virtual test bench

A virtual test bench was implemented using API interface in Abaqus to automate the creation of laminate geometry featuring graded waviness and further build up of FE model for coupon simulations. The wavy geometry is based on equation of a sinusoidal wave and amplitude  $\delta$  and defect length  $l$  of the waviness in the topmost ply is used to derive the coordinates for sketching Spline 1 and Spline 2 in Abaqus (as shown in Fig. 8). The test bench prepares FE descriptions of coupon with following geometric parameters: width, gauge length, laminate thickness and cohesive thickness, the layup definition: number of layers and the configuration, the defect geometry: defect length and amplitude, the simulation parameters: velocity, end time, number of data points and mesh size and finally the material parameters.

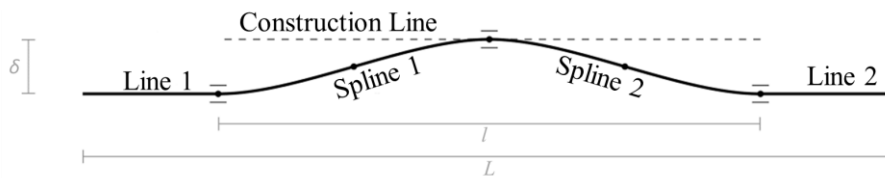


**Figure 8.** Wave sketch generation

### 3.1.3 Results

The simulation results of undisturbed specimen ( $\delta/l=0.0$ ) under tension as expected showed progressive failure of plies with matrix failure under tension of  $90^\circ$  plies at around 0.15mm displacement and the matrix failure of  $\pm 45^\circ$  plies starting at around 0.22 mm which leads to dip in the force displacement curve until the fiber failure of  $0^\circ$  plies under tension at 0.4 mm which leads to ultimate laminate failure. The comparison of FD-curves between undisturbed laminates and laminates featuring graded waviness (Fig. 9 and Fig. 10) show that there is a prominent drop in the load bearing capacity of the latter. The maximum load of variants with flange angles of  $150^\circ$  ( $\delta/l=0.065$ ) and  $135^\circ$  ( $\delta/l=0.243$ ) drop by about 25% and 66% respectively. In the former variant the onset of damage is due



to mode 2 delamination between undulated plies and it starts at displacement of 0.11 mm. The first ply failure of bottommost 90° ply happens at 0.14 mm. For the latter variant the damage onset is due to mode 1 delamination of the cohesive elements between the two topmost plies at 0.034 mm. . The first ply failure of bottommost 90° ply happens at 0.12 mm. In both the cases the failure progression is the same wherein the bottommost plies are initially the load bearers until they collapse and transfer the load to next plies above and this load transfer and failure progression process continues until the failure topmost ply with maximum waviness amplitude. Incase of 150° variant, the failue progression is rapid as the difference of defect amplitude between plies is relatively small. But incase of 135° variant the the failure progression is slower and this leads to cascading force displacement curve. The Fig. 9 and 10 also show the ply stress in the fiber direction of 0° plies.

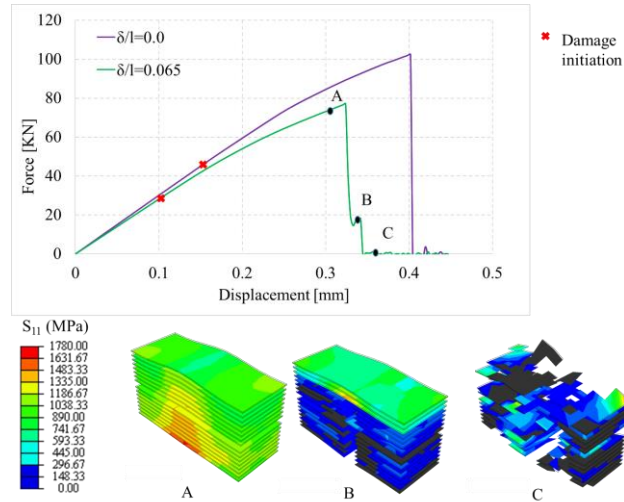


**Figure 9.** Force displacement curve for static tension load case: Undisturbed laminate ( $\delta/l=0.0$ ) versus laminate featuring graded waviness ( $\delta/l=0.065$ ). Contour plots show ply stress in fiber direction in the latter specimen.

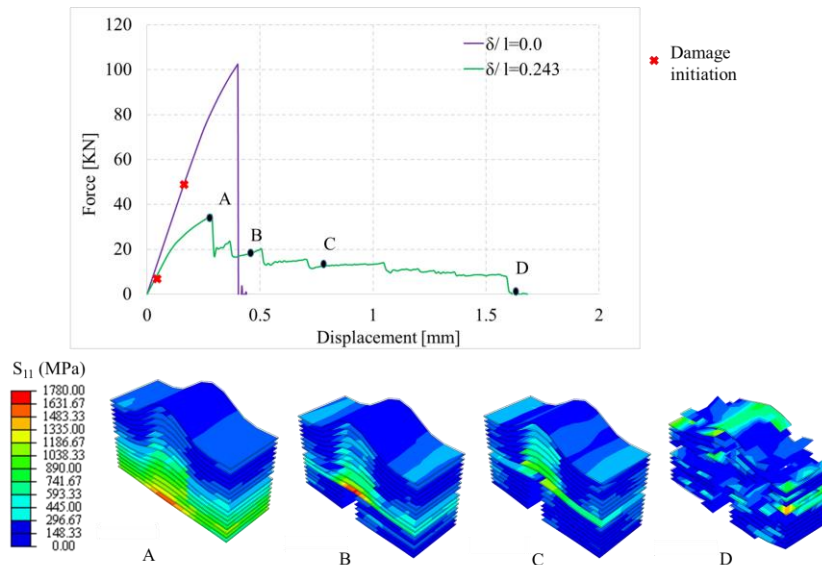


**Figure 10.** Force displacement curve for static tension load case: Undisturbed laminate ( $\delta/l=0.0$ ) versus laminate featuring graded waviness ( $\delta/l=0.243$ ). Contour plots show ply stress in fiber direction in the latter specimen.

The simulation results of undisturbed specimen under compression show that all the plies fail simulataneously at about 0.24 mm although the damage onset is due to mode 1 delamination between central plies at 0.2 mm. Like in the case of tension test there is also a drop of maximum load carried by

laminates featuring waviness. The maximum load of the specimens featuring waviness drop by about 34% (for  $\delta/l=0.065$ ) and 62% (for  $\delta/l=0.243$ ) respectively (Fig. 11 and 12). The onset of damage in the former specimen is due to mode 2 delamination between undulated plies and it starts at displacement of 0.11 mm. For the variant with flange angle of  $135^\circ$  the damage onset is due to mode 1 delamination of the cohesive elements between the two topmost plies at 0.042 mm. In case of specimens with waviness, the plies at the bottom which are aligned along the loading direction fail when their compressive strength is reached. But the upper plies with undulations tend to bend towards the defect direction. This bending leads eventually to instable and catastrophic delamination failure between the plies. In case of laminates with higher waviness amplitude like  $135^\circ$  variant (Fig. 12) this ultimate laminate failure occurs earlier due to severity of the waviness but in case of  $150^\circ$  variant (Fig. 11) the laminate bends for a longer time before the ultimate failure occurs as indicated by the gradual drop in force value.

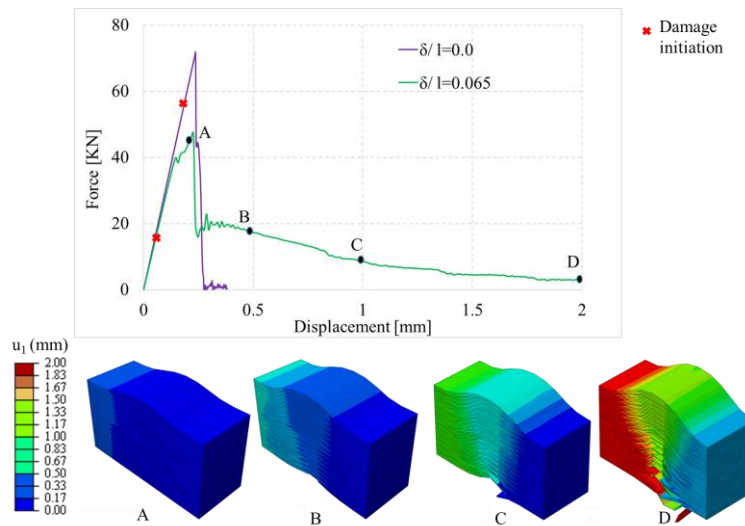


**Figure 11.** Force displacement curve for static compression load case: Undisturbed laminate ( $\delta/l=0.0$ ) versus laminate featuring graded waviness ( $\delta/l=0.065$ ). Contour plots show displacement in the loading direction in the latter specimen.

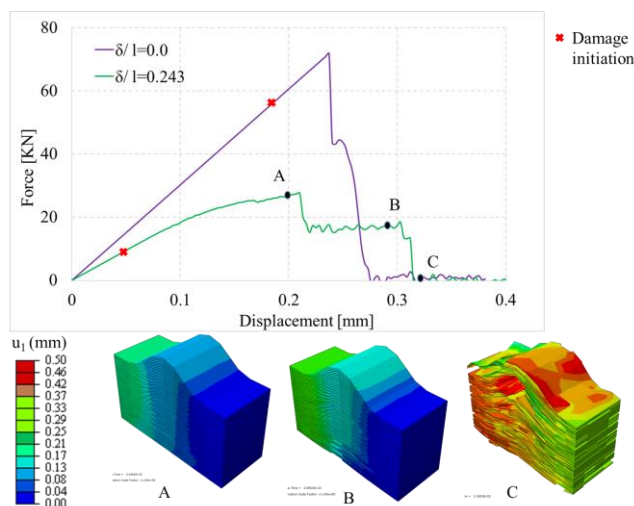


**Figure 12.** Force displacement curve for static compression load case: Undisturbed laminate ( $\delta/l=0.0$ ) versus laminate featuring graded waviness ( $\delta/l=0.243$ ). Contour plots show displacement in the loading direction in the latter specimen.



#### 4. Conclusions

This study proposes two methods of controlled defect introduction in a composite laminate in terms of ply undulations. A temporary insertion of a rod to cause a layer to fold or wrinkle has been used to introduce this defect type on a single layer of the laminate. The bent plate method has been developed for creating laminates featuring out-of-plane waviness with a maximum amplitude of the wave at the topmost ply and reducing amplitude of the subsequent plies till it vanishes at bottommost ply. Both methods have a simple setup and proved reproducible. The defect severity or dimensions can be varied in these methods by changing the rod diameter and the flange angle of the bent plate tool respectively.

A so called fine modelling technique is used to simulate the static tensile and compression tests wherein each ply is modeled individually using an anisotropic damage model for composites in Abaqus and the interface delamination is predicted using cohesive elements which are modeled using a traction-separation law. A virtual test bench is presented which has been used to automate the creation of specimen geometries with defects and to derive representative FE models for coupon simulations. The simulation of tensile tests as expected predicted the progressive ply failure from the bottom plies to the top with cascading nature of the force displacement curve for severe defects. The simulation of compression tests also predicted the bending induced delamination failure at the ply interfaces.

Subsequently physical tests are to be carried out on coupons of undisturbed and undulated ply configurations in order to validate results on the load bearing behavior derived from the virtual testbench.

#### Acknowledgments

The authors acknowledge AIRBUS for funding this work within the framework of the project 'Next Move'. The authors would like to thank Mr. Wolfgang Machunze and Mr. Jörn Ewald from AIRBUS for their inputs and support within this research.

#### References

- [1] T.J. Dodwell, R. Butler and G. W. Hunt, Out-of-plane ply wrinkling defects during consolidation over an external radius. *Composites Science and Technology*, 105: 151–159, 2014.
- [2] D. Kugler, T.J. Moon, Identification of the most significant processing parameters on the development of fiber waviness in thin laminates. *Journal of Composite Materials*, 36(12) : 1451-1479, 2002.
- [3] M.R. Wisnom, J. W. Atkinson, Fiber waviness generation and measurement and its effect on compressive strength. *Journal of reinforced plastics and composites*, 19 (2): 96-110, 2000
- [4] J. Wang, K.D Potter, K. Hazra and M.R. Wisnom, Experimental fabrication and characterization of out-of-plane fiber waviness in continuous fiber-reinforced composites. *Journal of Composite Material*, 0(0): 1-13, 2012.
- [5] H.-J. Chun, J.-Y. Shin and I. M. Daniel, Effects of material and geometric nonlinearities on the tensile and compressive behavior of composite materials with fiber waviness. *Composite Science and Technology*, 61: 125-134, 2001.
- [6] S. Hörmann, A. Adumitroaie, M. Schagerl, The effect of ply folds as manufacturing defect on the fatigue life of CFRP materials. *Frattura ed Integrità Strutturale*, 38: 76-81, 2016.
- [7] D. O'H. Adams, M. W. Hyer, Effects of layer waviness on the compression strength of thermoplastic composite laminates.
- [8] T. A. Bogetti, J. W. Gillespie Jr., M. A. Lamontia, The influence of ply waviness with non-linear shear on the stiffness and strength reduction of composite laminates. *J. Thermoplastic Composite Materials.*, 7: 76-90, 1994. 12: 414-429, 1993.

- [9] H. M. Hsaio, I. M. Daniel, Effect of fiber waviness on stiffness and strength reduction of unidirectional composites under compressive loading. *Composite Science and Technology*, 56(5): 581-593, 1996.
- [10] M. R. Garnich, G. Karami, Finite element micromechanics for stiffness and strength of wavy fiber composites. *Journal of Composite Materials*, 38(4): 273-292, 2004.
- [11] S. L. Lemanski, J. Wang, M. P. F. Sutcliffe, K. D. Potter and M. R. Wisnom, Modeling of failure of composite specimens with defects under compression loading. *Composite Part A: Applied Science and Manufacturing*, 38(11): 2333-2341, 2007.
- [12] P. Duangman, Layer waviness effects on compression strength of composite laminates: Progressive failure analysis and experimental validation, Phd. Dissertation, The University of Utah, 2012.
- [13] J.S. Sun, K.H. Lee, H.P. Lee, Comparison of implicit and explicit finite element methods for dynamic problems, *Journal of Material Processing Technology*, 105: 110-118, 2000.
- [14] ASTM Interntional, ASTM D6641 / D6641M-01e1, Standard Test Method for Compressive Properties of Polymer Matrix Composite Materials Using a Combined Loading Compression (CLC) Test Fixture, 2016.
- [15] ASTM Interntional, ASTM D3039 / D3039M-17, Standard Test Method for Tensile Properties of Polymer Matrix Composite Materials, 2017.
- [16] A. P. J. Altmann, Matrix dominated effects of defects on the mechanical properties of wind turbine blades. Dissertation, Technical University of Munich, Munich, 2015.
- [17] Abaqus Analysis Users' Manual. Version 6.17. Dassault Systèmes; 2017.
- [18] A. Matzenmiller, J. Lubliner, R. L. Taylor, A Constitutive Model for Anisotropic Damage in Fiber-Composites, *Mechanics of Materials*, 20: 125–152, 1995.
- [19] P. P. Camanho, C. G. Dávila, Mixed-Mode Decohesion Finite Elements for the Simulation of Delamination in Composite Materials, *NASA/TM*, 1-37, 2002.
- [20] Z. Hashin, A. Rotem, A Fatigue Criterion for Fiber-Reinforced Materials, *Journal of Composite Materials*, 7: 448–464, 1973.
- [21] Z. Hashin, Failure Criteria for Unidirectional Fiber Composites, *Journal of Applied Mechanics*, 47: 329–334, 1980.
- [22] M. Hoffmann, K. Zimmermann, P. Mittendorf, Determination of through thickness strength properties to predict the failure of thick-walled composite lugs, *20th International Conference on Composite Materials Copenhagen*, 2005.
- [23] M. L. Benzeggagh, M. Kennane, Measurement of mixed-mode delamination fracture toughness of unidirectional glass/epoxy composites with mixed-mode bending apparatus, *Composites Science and Technology*, 56(4): 439-449, 1996.
- [24] A. Turon, C. G. Dávila, P. P. Camanho, J. Costa, An engineering solution for solving mesh size effects in the simulation of delamination with cohesive zone models, *NASA Technical Reports*, 2005